Chinese Journal of Polymer Science Vol. 33, No. 9, (2015), 1294–1304

Chinese Journal of Polymer Science

Phase Morphology, Crystallization Behavior and Mechanical Properties of Poly(L-lactide) Toughened with Biodegradable Polyurethane: Effect of Composition and Hard Segment Ratio*

Qian Xing[a, b], Rong-bo Li[c], Xia Dong[b**], Xiu-qin Zhang[b], Liao-yun Zhang[a] and Du-jin Wang[b]

[a] *School of Chemistry and Chemical Engineering, University of Chinese Academy and Sciences, Beijing 100049, China*

[b] *Beijing National Laboratory for Molecular Sciences, CAS Key Laboratory of Engineering Plastics, Institute of Chemistry, Chinese Academy of Sciences, Beijing 100190, China*

[c] *Petrochina Petrochemical Research Institute, Beijing 100195, China*

Abstract Polyester-based biodegradable polyurethane (PU) with different hard segment ratios was selected to modify the impact toughness of poly(L-lactide) (PLLA). The influence of blending composition and hard segment ratio of PU on the phase morphology, crystallization behavior and mechanical properties of PLLA/PU blends has been investigated systematically. The results showed that the PU particles were uniformly dispersed in PLLA matrix at a scale from sub-microns to several microns. The glass transition temperature of PU within these blends decreased compared to that of neat PU, but rose slightly with its content and hard segment ratio. The presence of PU retarded the crystallization ability of PLLA, whereas enhanced its elongation at break and impact resistance effectively. As the PU content reaches up to 30 wt%, the phenomenon of brittle-ductile transition occurred, resulting in a rougher fracture surface with the formation of fibril-like structure. Moreover, under the same concentrations, the elongation at break and impact strength of PLLA blends decreased slightly with the increase of hard segment ratio of PU.

Keywords: Poly(L-lactide); Polyurethane; Phase morphology; Impact modification; Hard segment ratio.

INTRODUCTION

As an eco-friendly thermoplastic polyester, poly(L-lactide) (PLLA) has been widely used in biomedical applications such as surgical sutures and controlled drug delivery systems, owing to its excellent biodegradability and biocompatibility[1–5]. Moreover, PLLA possesses good rigidity and thermoplastic process ability, and can act as a suitable alternative to some traditional petrochemical-based polymers in the fields of food packaging, textile and clothing[6–8], *etc*, However, the glass transition of PLLA generally occurs around 60 °C, below which it appears hard and brittle. Therefore, the impact resistance of as-processed PLLA products is generally very poor at room temperature, which consequently limits its extensive application.

To date, there have been considerable researches devoted to improving the impact toughness of PLLA, such as graft and block copolymerization as well as physical blending with a second polymer[9–18], *etc*. In particular, the method of physical blending can be envisaged as a relatively economical and practical manner to modify the physic-mechanical properties of polymers[19–24]. It has been reported that a variety of flexible polymers can be

* This work was financially supported by the National Natural Science Foundation of China (No. 51403210), China Postdoctoral Science Foundation (No. 2014M550801) and President Fund of University of Chinese Academy of Sciences (No. Y35102CN00).

** Corresponding author: Xia Dong (董侠), E-mail: xiadong@iccas.ac.cn

Received January 31, 2015; Revised April 1, 2015; Accepted April 3, 2015
doi: 10.1007/s10118-015-1679-y

used to toughen PLLA, including polyethylene (PE), acrylonitrile-butadiene-styrene copolymer (ABS), and poly(ethylene oxide) (PEO)[14–16], *etc*. However, these traditional petrochemical-based polymers are not biodegradable, and blending with them would deteriorate the environment friendliness of PLLA. Fortunately, the fully biodegradable aliphatic polyesters, such as poly(ε-caprolactone) (PCL) and poly(butylene succinate) (PBS)[17, 18], have been suitable alternative polymers to toughen PLLA. In most cases, the second polymer within the blends is incompatible with PLLA matrix, which would induce the macroscopic phase separation, resulting in poor toughening effect. At the same time, the rigidity of PLLA blends would decrease generally during the modification of impact toughness. Therefore, it has been drawing great attention to improve the compatibility of different components in polymer blends by employing suitable compatibilizer[15, 17, 18, 25]. Li *et al*.[15] found that the addition of ABS cannot enhance the impact toughness of PLLA effectively due to the thermodynamic immiscibility of PLLA and ABS. They adopted the reactive styrene/acrylonitrile/glycidyl methacrylate copolymer (SAN-GMA) as the *in situ* compatibilizer for PLLA/ABS blends, and thus a better stiffness-toughness balance has been achieved. Semba *et al*.[17] promoted the interfacial adhesion between PLA and PCL by the crosslinking reaction with the aid of dicumyl peroxide, which resulted in the remarkable decrease of the dispersed PCL domains and increase of tensile strain from 15% to 130%.

Thermoplastic polyurethane (PU), as an important elastomer, has great potential application in diverse areas such as automobile and medical devices[26–28], owing to the combination of high toughness, good biocompatibility, biostability and bioactivity. The main chain of PU is generally composed of thermodynamically incompatible hard and soft segments. The soft segments are usually polyether or polyester with a high flexibility at room temperature, whereas the hard segments consist of diisocyanate and a low-molecular-weight diol (chain extender), which particularly provides the high modulus, hardness and tear strength. There are many polar groups along the backbones of PU, including －NH and －C＝O groups, which are assumed to have interaction with the －C＝O groups within PLLA chains and thus enhances the compatibility between PLLA and PU. Therefore, PU has been adopted to mediate the impact resistance as well as other physical properties of PLLA[29–32].

In addition, the intermolecular interaction of PU molecules can be altered through adjusting the hard segment ratio[33], which may produce great effect on the interaction between PU and PLLA. It arouses our great interest what would happen when PU with different hard segment ratios is added into PLLA? Therefore, in present study, polyester-based PU with four kinds of hard segment ratios was selected to blend with PLLA so as to obtain PLLA/PU blends with increased impact resistance and maintaining biodegradability. The specific objective was to illustrate the influence of the content and hard segment ratio of PU on the phase morphology, crystallization behavior and mechanical properties of PLLA.

EXPERIMENTAL

Materials

PLLA of commercial grade 2002D with 4.6 wt% of D-isomer units was purchased from NatureWorks. The number and weight average molecular weights are 1.5×10^5 g/mol and 2.0×10^5 g/mol, respectively. Four polyester-based PUs with different hard segment ratios were kindly supplied by Wanhua Chemical Group Co., Ltd. (Yantai, China). As shown in Scheme 1, the soft segment of these PUs is PCL, while the hard segment is －$CONHC_6H_4CH_2C_6H_4NHCOO(CH_2)_4O$－, obtained through the reaction of MDI and BDO. The hard segment ratio in the increase sequence is 32 wt%, 36 wt%, 41 wt% and 44 wt% for PU1, PU2, PU3 and PU4, respectively. The received materials were dried in a vacuum oven for 24 h at 70 °C and then stored in a desiccator before use.

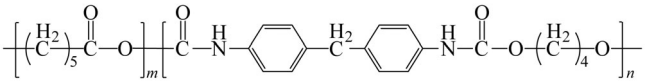

Scheme 1 Chemical structure of PU

Sample Preparation

Two series of PLLA/PU blends were prepared through melt mixing by using HAAKE PolyLab OS at 190 °C and 60 r/min. For PLLA/PU1 blends, the content of PU1 varied from 1 wt% to 30 wt% and the samples were denoted as PU1-x, where x represents the weight percent of PU1. For PLLA/PU (80/20) blends, the PU with different hard segment ratios were also blended with PLLA with a fixed content of 20 wt%, which were named as PU1-20, PU2-20, PU3-20 and PU4-20.

Characterizations

The dispersion of PU in PLLA was examined with a JSM-6700F (JEOL) scanning electron microscope (SEM) operated at an acceleration voltage of 5 kV. The samples were cryo-fractured in liquid nitrogen and a platinum layer was deposited on the cross sections prior to SEM observation. The impact fractured surfaces were also observed with the same method.

The crystallization behavior of PLLA and PLLA/PU blends were measured on a DSC-7 differential scanning calorimeter (Perkin-Elmer). The temperature and heat flow were calibrated by using indium as the standard. The measurement was conducted under nitrogen atmosphere. Samples about 5 mg were weighed and sealed in an aluminum pan, heated to 200 °C and held for 3 min to eliminate the thermal history. During the non-isothermal crystallization, the samples were first cooled from 200 °C to 50 °C at 2 K/min and then heated to 200 °C at 10 K/min. In the isothermal crystallization, samples were quenched from 200 °C to 105 °C at 30 K/min and held at this temperature until the samples crystallized completely.

The tensile stress at yield and elongation at break of pure PLLA and PLLA/PU blends were measured at room temperature with an Instron 3365 universal materials testing machine, according to ISO 527-2:1993. The crosshead speed was set as 50 mm/min. The data were averaged for at least five independent measurements. The notched Izod impact strength was measured on a Ceast pendulum impact strength tester (CSI-137C) at 23 °C, according to ISO 180:2000. The drop velocity was 3.5 m/s and the testing results were the average of ten parallel experiments. All the specimens for mechanical tests were prepared by injection molding at 190 °C.

Dynamic mechanical analysis (DMA) was carried out with a Q800 dynamic mechanical analyzer (TA Instruments) in the tensile mode. The hot pressed rectangle specimens were adopted with the size of 14 mm × 4 mm × 0.1 mm (length × width × thickness). The amplitude of 25 μm was selected by means of a strain sweep test to ensure that the experiments were conducted in the linear viscoelastic region. The dynamic storage modulus (E'), loss modulus (E'') and tangent of loss angle tanδ (= E''/E') were determined at a frequency of 1 Hz and a heating rate of 3 K/min from −145 °C to 150 °C.

RESULTS AND DISCUSSION

Phase Morphology and Miscibility

For polymer blends, the domain size and size distribution of dispersed phases as well as the interfacial adhesion play important roles in determining the actual mechanical properties. Therefore, it is essential to fully understand the phase morphology of PLLA/PU blends and its correlation with mechanical properties. SEM images for the cryo-fractured surfaces of neat PLLA and PLLA/PU1 blends are shown in Fig. 1. It can be seen that the spherical PU1 particles are evenly dispersed in PLLA matrix, forming typical “sea-island” structure in the binary system. The size of the dispersed PU1 particles maintains at a scale of sub-microns under lower PU1 content (< 20 wt%), while still remains in between 1–2 μm as the content reaches 30 wt%. The PU domains at such scale are suitable to promote the shear yielding and plastic deformation of PLLA matrix under external forces[34, 35].

SEM images for the cryo-fractured surfaces of PLLA/PU (80/20) blends containing PU with different hard segment ratios are shown in Fig. 2. It can be seen that the size and size distribution of the PU particles decrease slightly with the increase of hard segment ratio. PU particles in PU1-20 and PU2-20 possess a diameter in between 1–2 μm, while those in PU3-20 and PU4-20 decrease to a scale of sub-microns.

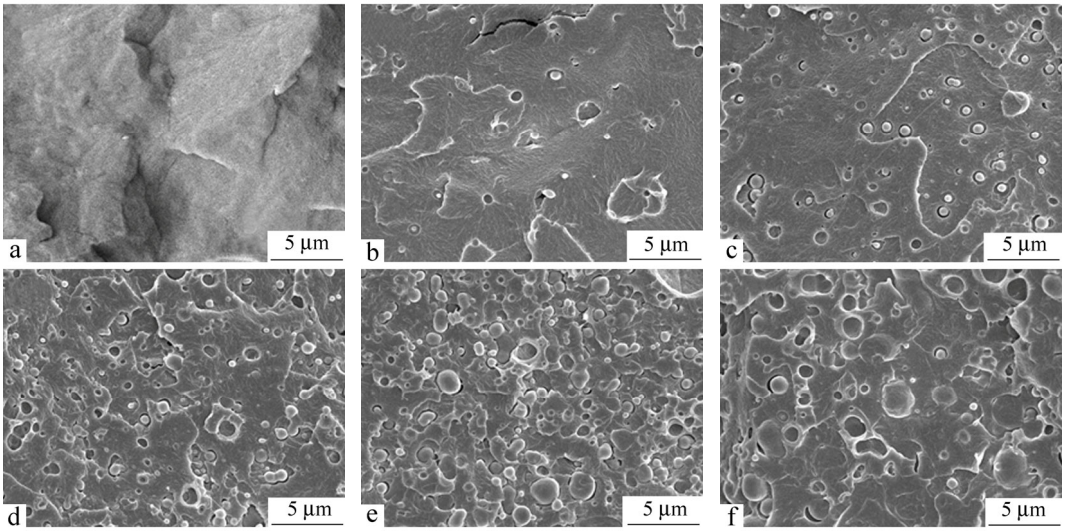

Fig. 1 SEM images for the cryo-fractured surfaces of neat PLLA and PLLA/PU1 blends: (a) Neat PLLA, (b) PU1-1, (c) PU1-5, (d) PU1-10, (e) PU1-20 and (f) PU1-30

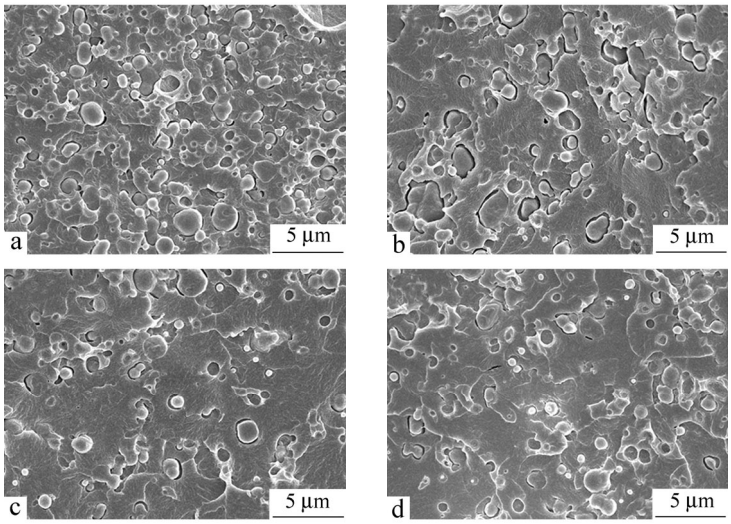

Fig. 2 SEM images for the cryo-fractured surfaces of PLLA/PU (80/20) blends: (a) PU1-20, (b) PU2-20, (c) PU3-20 and (d) PU4-20

The dynamic viscoelastic curves of tanδ versus temperature of pristine polymers and PLLA/PU blends are shown in Fig. 3. Each pristine polymer shows one obvious glass transition peak, which appears around 60 °C and −30 °C for neat PLLA and PU1, respectively. All the PLLA/PU blends exhibit two distinguished glass transition domains, indicating the immiscibility of PLLA and PU. For PLLA/PU1 blends, the glass transition temperature (T_g) of neat PLLA remains almost constant with the content of PU1, while that of PU1 shifts to lower temperatures. This implies that the PU1 molecules may interact with the adjacent PLLA molecules and the partial interfacial compatibility may exist. According to the chemical structure of PLLA and PU1, it is supposed that such interchain interaction may be ascribed to the hydrogen-bonding interaction between the －NH groups within the hard segments of PU1 and the －C＝O groups of PLLA. Tien *et al.*[36] also found the existence of hydrogen-bonding interaction between the －OH groups on the nanometer-scale silicate layers and the hard or the soft segments of PU, which thus reduced the hydrogen-bonding interaction between the hard segments of PU. Meanwhile, the T_g of PU1 increases slightly with the increase of PU1 content and gradually approaches to

that of neat PU1. Otherwise, the presence of PU1, as the minor dispersion phase of the blend, has little influence on the glass transition behavior of PLLA matrix. For PLLA/PU (80/20) blends, the T_g of PU in the blends increases with the increase of its hard segment ratio, due to the increase of the hydrogen-bonding interaction between the hard segments of PU.

As a matter of fact, there are two kinds of competitive interchain interactions existing in these binary systems. The one is between the hard segments of PU, while the other one is between the hard segments of PU and PLLA. Both of the interactions may be proportional to the hard segment ratio of PU. The unchanged T_g of PLLA reveals that the interchain interaction between the hard segments of PU plays a dominant role in these blends and is stronger than that between PLLA and PU. Therefore, the PU molecules are prone to coalesce into small domains acting as "islands" in PLLA matrix. Otherwise, the probable interaction between PLLA and PU enhances the mobility of PU and leads to the decrease of its glass transition temperature.

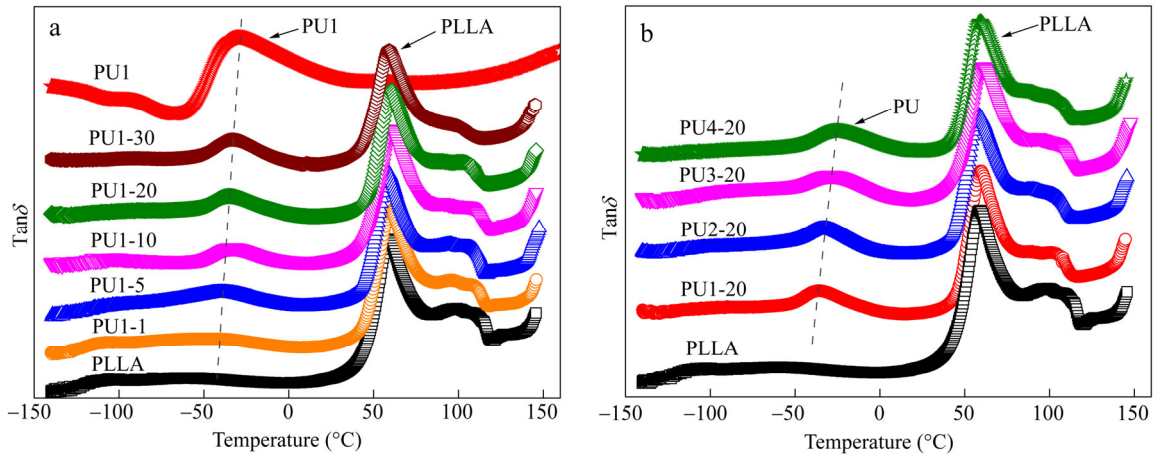

Fig. 3 Dynamic viscoelastic curves of tanδ versus temperature for PLLA/PU1 blends (a) and PLLA/PU (80/20) blends (b)

Crystallization Behavior

DSC heating curves at 10 K/min for neat PLLA and PLLA/PU blends are shown in Fig. 4, and the crystallization parameters are listed in Table 1. It can be observed that an obvious heat relaxation corresponding to the glass transition of PLLA appears around 60 °C, which can be attributed to the rearrangement of amorphous molecular chains of PLLA. During the heating process, the cold crystallization of neat PLLA occurs at about 127.8 °C with a cold crystallization enthalpy (ΔH_{cc}) of 1.1 J/g. The addition of 1 wt% PU1 has no evident influence on the cold crystallization behavior of PLLA. With the further increase of PU1 content, the cold crystallization of PLLA was postponed to occur at higher temperatures and the value of ΔH_{cc} was decreased. In terms of PLLA/PU (80/20) blends, the addition of PU with higher hard segment ratios exhibit similar effect on the crystallization behavior as PU1, leading to the increase of T_{cc} and the decrease of ΔH_{cc}.

Table 1. DSC parameters for neat PLLA and PLLA/PU blends during the non-isothermal crystallization

Samples	T_{cc} (°C)	ΔH_{cc} (J/g)	T_m (°C)	ΔH_m (J/g)
PLLA	127.8	1.1	151.5	3.1
PU1-1	127.5	1.2	150.9	3.1
PU1-5	129.3	0.1	150.9	1.2
PU1-10	128.9	0.7	150.8	1.9
PU1-20	129.0	0.3	150.9	1.7
PU1-30	129.8	0.8	150.9	2.3
PU2-20	129.0	0.2	150.9	1.1
PU3-20	128.9	0.4	150.9	1.5
PU4-20	129.8	0.2	150.8	1.6

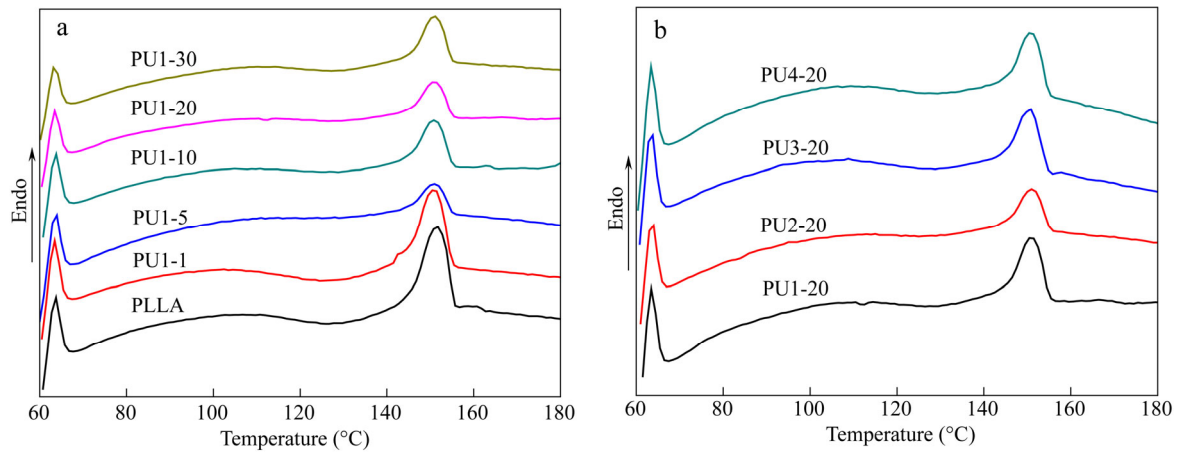

Fig. 4 DSC heating curves at 10 K/min for PLLA/PU1 blends (a) and PLLA/PU (80/20) blends (b)

The isothermal crystallization traces of neat PLLA and its PU blends at 105 °C are shown in Fig. 5. It can be noted that all the samples show obvious crystallization peaks and the overall crystallization time of PU-doped PLLA is much longer than that of neat PLLA, confirming that the presence of PU has decreased the isothermal crystallization rate of PLLA.

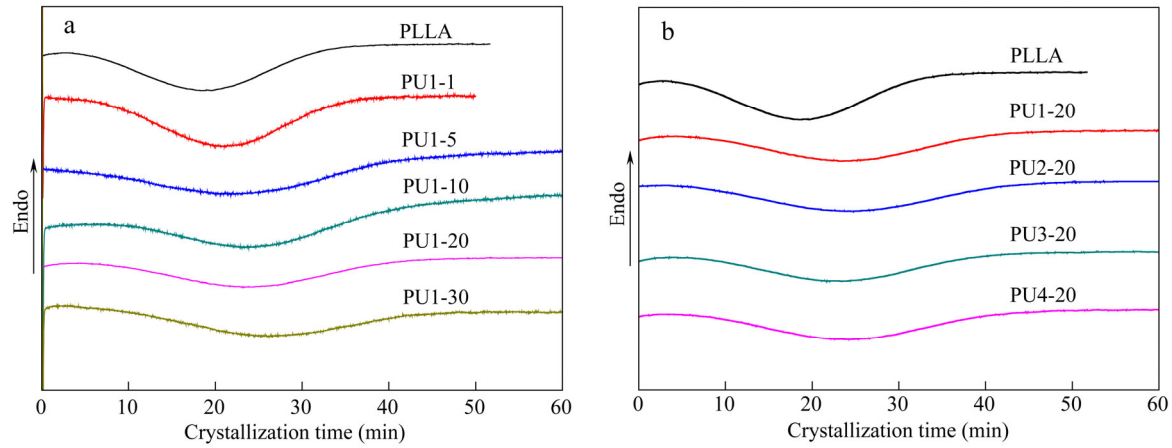

Fig. 5 DSC curves of neat PLLA and its PU blends isothermally crystallized at 105 °C: (a) PLLA/PU1 blends, (b) PLLA/PU (80/20) blends

The Avrami equation[37, 38] was employed to analyze the isothermal crystallization kinetics of PLLA and its PU blends, which describes the development of relative crystallinity (X_t) with crystallization time (t). The Avrami equation is written as:

$$1 - X_t = \exp(-Kt^n) \tag{1}$$

$$\ln[-\ln(1 - X_t)] = \ln K + n\ln t \tag{2}$$

where n is the Avrami index and K is the overall rate constant. As shown in Figs. 6(a1) and 6(b1), the time at which the relative crystallinity (X_t) of PLLA reaches 100% increases obviously with the addition of PU and the effects of different hard segment ratios are similar to each other. The Avrami plots in Figs. 6(a2) and 6(b2) show a good linear fitting for all the samples, and the values of n and K can be obtained from the slopes and the intercepts, respectively. The crystallization half-time ($t_{1/2}$), defined as the time when X_t reaches 50%, was

introduced for the analysis of the crystallization kinetics, calculated as Eq. (3):

$$t_{1/2}=(\frac{\ln 2}{K})^{1/n} \tag{3}$$

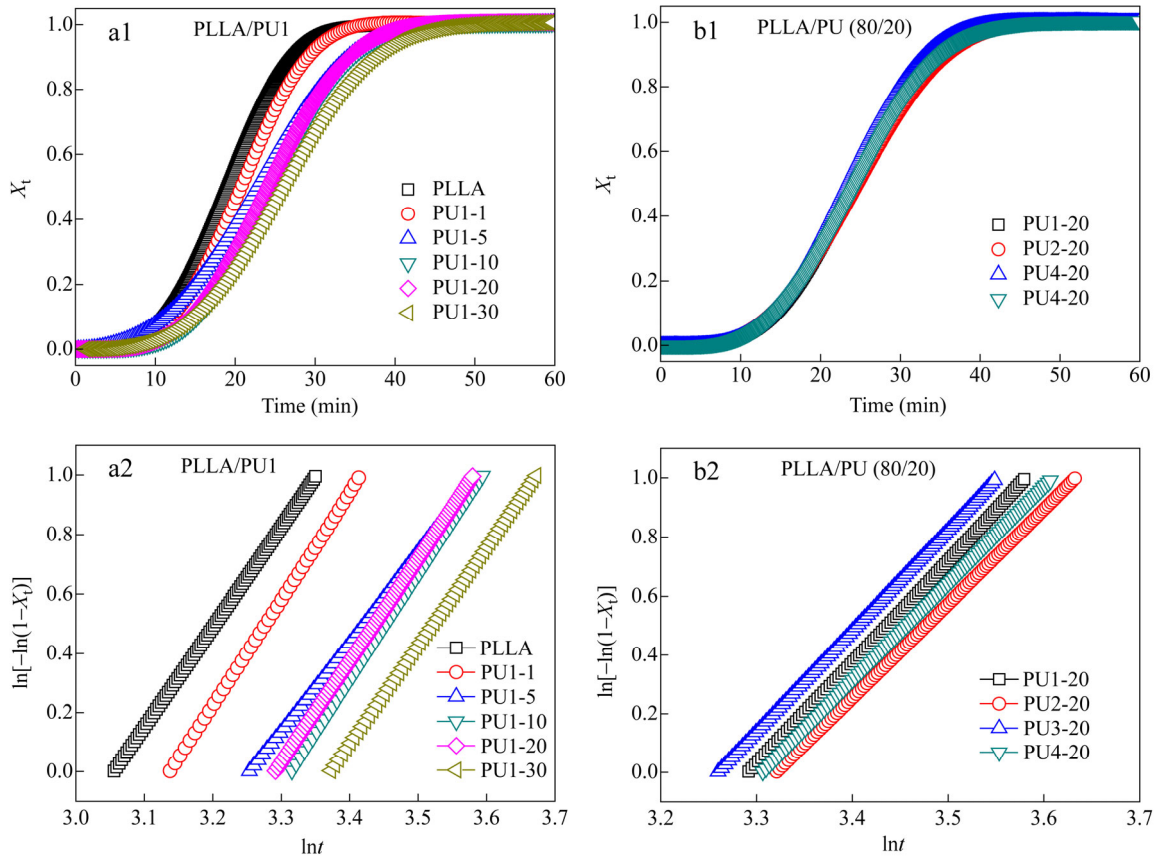

Fig. 6 The variation of relative crystallinity (X_t) versus crystallization time (a1, b1) and the Avrami plots (a2, b2) for PLLA/PU1 and PLLA/PU (80/20) blends isothermally crystallized at 105 °C

The isothermal crystallization kinetics parameters calculated by employing Avrami equation are listed in Table 2. The value of n varies between 3.0 and 3.6 for neat PLLA and all its PU blends, suggesting that the incorporation of PU does not change the three-dimentional heterogeneous nucleation mechanism of PLLA. On the other hand, the value of $t_{1/2}$ was increased due to the addition of PU with respect to neat PLLA, *i.e.*, the overall crystallization time of PLLA was prolonged. Besides, the value of $t_{1/2}$ increases with the increase of PU1 content, but remains nearly constant with different hard segment ratios of PU. Considering the non-isothermal crystallization behavior, it can be concluded that the addition of PU has retarded the crystallization of PLLA. This may be attributed to the weak interchain interaction between PLLA and PU, which depresses the nucleation and crystal growth of PLLA.

Mechanical Properties

The stress-strain curves and Izod impact strength of neat PLLA and PLLA/PU blends are shown in Figs. 7 and 8. Neat PLLA exhibits the best rigidity with a tensile stress at yield beyond 70 MPa, but the impact strength is only 2.1 kJ/m^2, resulting in a brittle fracture with the elongation at break below 5%. The addition of PU can effectively enhance the toughness of PLLA. For PLLA/PU1 blends, the shear yielding behavior begins to appear during the tensile testing with the addition of PU1, and subsequently the stress plateau of plastic deformation appears, where the strain develops continuously and the stress remains almost constant. As a result, the

elongation at break increases from 2% to 229% with the increase of PU content, while the impact strength increases from 2.1 kJ/m^2 to 40.0 kJ/m^2. It can be noted that the brittle-ductile transition takes place when the content of PU reaches 30%, as the elongation at break and the impact strength at this point rise abruptly. Based on Figs. 7(b) and 8(b), the increase of hard segment ratio in PU chains has no evident influence on the stress at yield, but produces negative effect on the elongation at break and the impact strength. DMA spectra have shown that the elevated hard segment ratio would lead to the enhancement of interaction between the adjacent hard segments, which would deteriorate the molecular mobility of PU chains. As a consequence, the toughening effect of PU would decrease with the increase of hard segment ratio.

Table 2. The Avrami parameters of PLLA and PLLA/PU blends during the isothermal crystallization at 105 °C

Samples	n	K ($\times 10^{-5}$ min^{-n})	$t_{1/2}$ (min)
PLLA	3.4	3.36	18.6
PU1-1	3.6	1.37	20.3
PU1-5	3.0	5.12	23.8
PU1-10	3.6	0.75	24.0
PU1-20	3.4	1.24	24.9
PU1-30	3.3	1.37	26.6
PU2-20	3.2	2.49	24.5
PU3-20	3.4	1.37	24.2
PU4-20	3.3	1.85	24.3

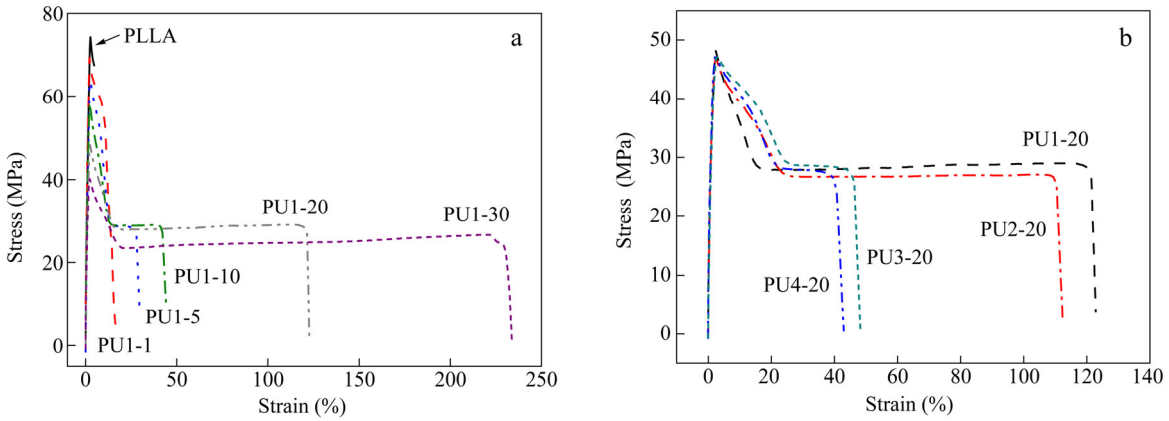

Fig. 7 Stress-strain curves for PLLA/PU1 blends (a) and PLLA/PU (80/20) blends (b)

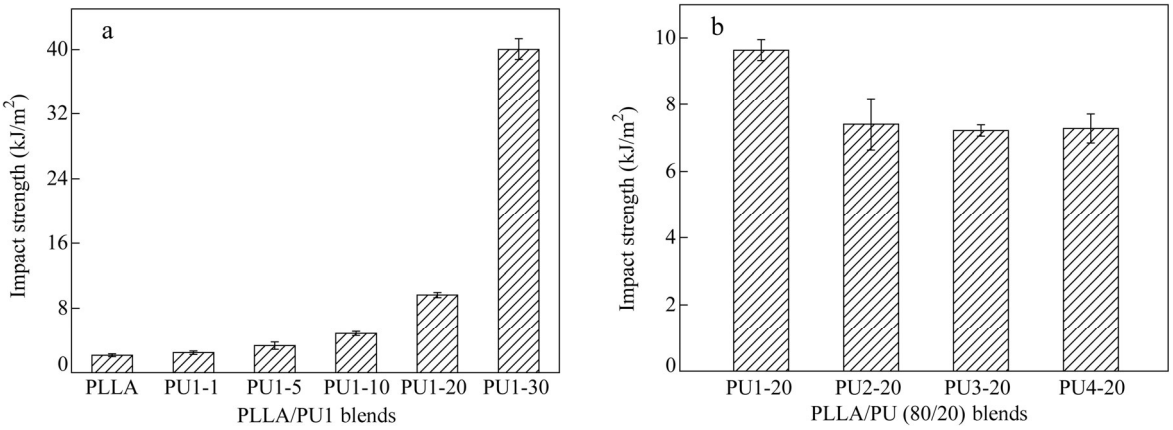

Fig. 8 Impact strength for PLLA/PU1 blends (a) and PLLA/PU (80/20) blends (b)

Fractographic observation on the impact fractured surface can provide useful information concerning deformation behavior of the PLLA/PU blends, as shown in Figs. 9 and 10. The fractured surface of neat PLLA appears very smooth (Fig. 9a), arising from the unstable crack propagation and brittle failure, which is well in accordance with its poor impact resistance. Since the addition of PU enhances the impact strength of PLLA, the phenomenon of stress whitening takes place during the impact measurement and the fractured surface becomes rougher with the increase of PU content. Moreover, some fibril-like structure can be observed for PU1-20 and PU1-30, as indicated by the white arrows. The formation of such fibril-like structure can absorb the impact energy, contributing to the impact toughness. Nevertheless, the PLLA/PU1 blends with lower PU1 content (≤ 20 wt%) still break in brittle fashion and only the sample of PU1-30 breaks in ductile manner. Due to the difference of elastic properties, the dispersed PU domains can act as stress concentration points in PLLA matrix.

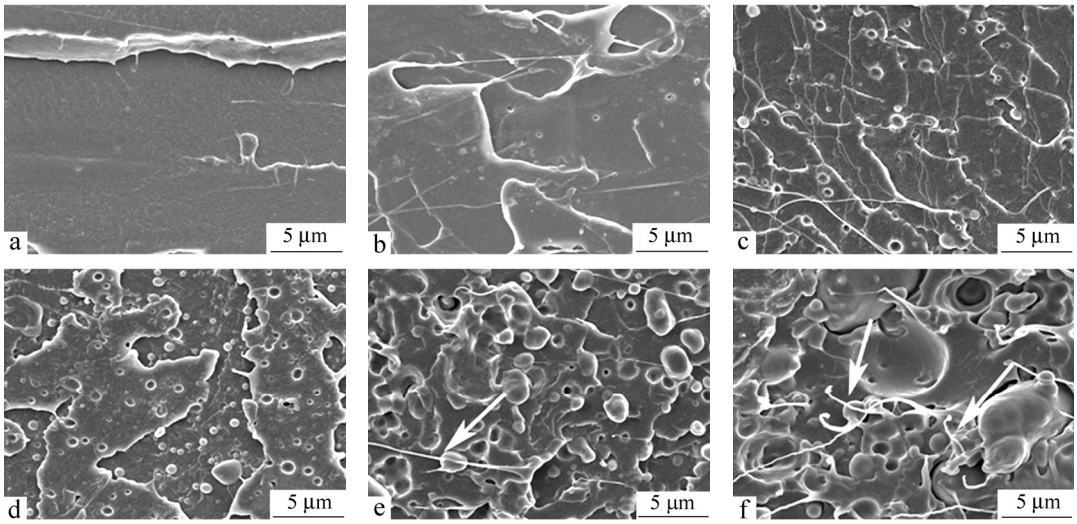

Fig. 9 SEM images for the impact fractured surfaces of neat PLLA and its PU1 blends: (a) Neat PLLA, (b) PU1-1, (c) PU1-5, (d) PU1-10, (e) PU1-20 and (f) PU1-30

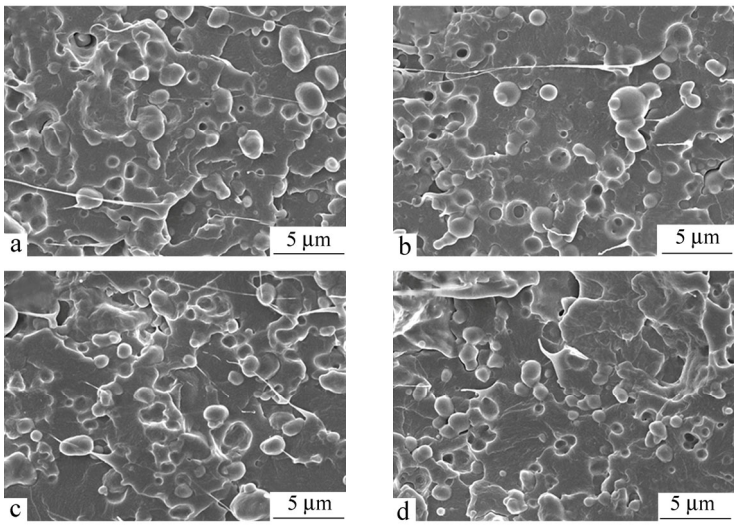

Fig. 10 SEM images for the impact fractured surfaces of PLLA/PU (80/20) blends: (a) PU1-20, (b) PU2-20, (c) PU3-20 and (d) PU4-20

When the PU1 content is below 20 wt%, the stress field around a PU particle is hardly affected by the surrounding ones due to the large interparticle distance. It's difficult in this case to induce the shear yielding and plastic deformation of PLLA. However, for PU1-30, the stress fields around neighboring particles would overlap and interact with each other owing to the decreased interparticle distance, promoting the generation of shear yielding and plastic deformation of PLLA matrix. The cooperative motion of the dispersed PU phases and PLLA matrix consumes large amount of energy and a transition to ductile behavior occurs.

Figure 10 indicates that the impact fractured surfaces of these PLLA/PU (80/20) blends are similar to each other. Comparatively, the sample of PU1-20 possesses a better impact toughness and generates more fibrils in its fractured surface. The above discussion has revealed that the interaction between the hard segments of PU is proportional to its hard segment ratio. Therefore, PU molecules with lower hard segment ratio would show a better mobility and toughening effect, compared to those with higher hard segment ratio.

CONCLUSIONS

In the present study, the effect of blending composition and hard segment ratio of PU on the phase morphology, crystallization behavior and mechanical properties of PLLA has been systematically evaluated. It has been found that the interchain interaction between PLLA and PU was beneficial to the homogeneous distribution of PU, and promoted the mobility of PU molecules with the decrease of glass transition temperature. Additionally, the glass transition temperature of PU increased slightly with the increase of its concentration and hard segment ratio. Moreover, the addition of PU depressed the crystallization kinetics of PLLA, but enhanced the break elongation and impact toughness of PLLA effectively. The enhancement degree of mechanical properties showed obvious dependence on the blending composition and the brittle-ductile transition occurred at a loading of 30 wt% PU. On the other hand, the increase of hard segment ratio of PU resulted in a slight decrease of break elongation and impact strength of PLLA.

REFERENCES

1 Garlotta, D., J. Polym. Environ., 2001, 9(2): 63
2 Ikada, Y. and Tsuji, H., Macromol. Rapid Commun., 2000, 21(3): 117
3 Nair, L.S. and Laurencin, C.T., Prog. Polym. Sci., 2007(8–9), 32: 762
4 Saeidlou, S., Huneault, M.A., Li, H. and Park, C.B., Prog. Polym. Sci., 2012, 37(12): 1657
5 Armentano, I., Bitinis, N., Fortunati, E., Mattioli, S., Rescignano, N., Verdejo, R., Lopez-Manchado, M.A. and Kenny, J.M., Prog. Polym. Sci., 2013, 38(10–11): 1720
6 Lim, L.T., Auras, R. and Rubino, M., Prog. Polym. Sci., 2008, 33(8): 820
7 Auras, R., Harte, B. and Selke, S., Macromol. Biosci., 2004, 4(9): 835
8 Drumright, R.E., Gruber, P.R. and Henton, D.E., Adv. Mater., 2000, 12(23): 1841
9 Sun, Y. and He, C., Macromolecules, 2013, 46(24): 9625
10 Martello, M.T. and Hillmyer, M.A., Macromolecules, 2011, 44(21): 8537
11 Wanamaker, C.L., Bluemle, M.J., Pitet, L.M., O'Leary, L.E., Tolman, W.B. and Hillmyer, M.A., Biomacromolecules, 2009, 10(10): 2904
12 Pezzin, A.P.T., van Ekenstein, G., Zavaglia, C.A.C., ten Brinke, G. and Deuk, E.A.R., J. Appl. Polym. Sci., 2003, 88(12): 2744
13 Afrifah, K.A. and Matuana, L.M., Macromol. Mater. Eng., 2010, 295(9): 802
14 Anderson, K.S., Lim, S.H. and Hillmyer, M.A., J. Appl. Polym. Sci., 2003, 89(14): 3757
15 Li, Y. and Shimizu, H., Eur. Polym. J., 2009, 45(3): 738
16 Gaikwad, A.N., Wood, E.R., Ngai, T. and Lodge, T.P., Macromolecules, 2008, 41(7): 2502
17 Semba, T., Kitagawa, K., Ishiaku, U.S. and Hamada, H., J. Appl. Polym. Sci., 2006, 101(3): 1816

18 Wang, R.Y., Wang, S.F., Zhang, Y., Wan, C.Y. and Ma, P.M., Polym. Eng. Sci., 2009, 49(1): 26
19 Wu, D.D., Li, W., Zhao, Y., Deng, Y.J., Zhang, H.L., Zhang, H.X. and Dong, L.S., Chinese J. Polym. Sci., 2015, 33(3): 444
20 Yang, T.B., Sun, X.L., Ren, Z.J., Li, H.H. and Yan, S.K., Chinese J. Polym. Sci., 2014, 32(9): 1119
21 Wang, G.Y. and Qiu, Z.B., Chinese J. Polym. Sci., 2014, 32(9): 1139
22 Wu, D.D., Li, W., Liang, H.Y., Liu, S.R., Fang, J.Y., Zhang, H.L., Zhang, H.X. and Dong, L.S., Chinese J. Polym. Sci., 2014, 32(7): 914
23 Zhang, S.M., Zhang, H.X., Zhang, W.Y., Wu, Z.Q., Chen, F. and Fu, Q., Chinese J. Polym. Sci., 2014, 32(7): 823
24 Pinijmontree, T. and Vao-soongnern, V., Chinese J. Polym. Sci., 2014, 32(5): 640
25 Na, Y.H., He, Y., Shuai, X., Kikkawa, Y., Doi, Y. and Inoue, Y., Biomacromolecules, 2002, 3(6): 1179
26 Chattopadhyay, D.K. and Webster, D.C., Prog. Polym. Sci., 2009, 34(10): 1068
27 Madbouly, S.A. and Otaigbe, J.U., Prog. Polym. Sci., 2009, 34(12): 1283
28 Petrović, Z.S. and Ferguson, J., Prog. Polym. Sci., 1991, 16(5): 695
29 Xing, Q., Dong, X., Li, R.B., Yang, H.J., Han, C.C. and Wang, D.J., Polymer, 2013, 54(21): 5965
30 Li, Y. and Shimizu, H., Macromol. Biosci., 2007, 7(7): 921
31 Feng, F. and Ye, L., J. Appl. Polym. Sci., 2011, 119(5): 2778
32 Feng, F., Zhao, X. and Ye, L., J. Macromol. Sci., B, 2011, 50(8): 1500
33 McKiernan, R.L., Heintz, A.M., Hsu, S.L., Atkins, E.D.T., Penelle, J. and Gido, S.P., Macromolecules, 2002, 35(10): 6970
34 Stehling, F.C., Huff, T., Speed, C.S. and Wissler, G., J. Appl. Polym. Sci., 1981, 26(8): 2693
35 Jang, B.Z., Uhlmann, D.R. and Sande, J.B.V., J. Appl. Polym. Sci., 1985, 30(6): 2485
36 Tien, Y.I. and Wei, K.H., Polymer, 2001, 42(7): 3213
37 Avrami, M., J. Chem. Phys., 1939, 7(12): 1103
38 Avrami, M., J. Chem. Phys., 1940, 8(2): 212